Carbohydrate Polymers 102 (2014) 699–707

Contents lists available at ScienceDirect

Carbohydrate Polymers

journal homepage: www.elsevier.com/locate/carbpol

Red emissive cross-linked chitosan and their nanoparticles for imaging the nucleoli of living cells

Ke Wang[a], Xun Yuan[a], Zhenpeng Guo[a,b], Jiying Xu[a,b], Yi Chen[a,b,*]

[a] Key Laboratory of Analytical Chemistry for Living Biosystems, Institute of Chemistry, Chinese Academy of Sciences, Beijing 100190, China
[b] Beijing National Laboratory for Molecular Science, Beijing 100190, China

ARTICLE INFO

Article history:
Received 1 September 2013
Received in revised form 23 October 2013
Accepted 31 October 2013
Available online 8 November 2013

Keywords:
Preparation
Chitosan
Red luminescence
Nanoparticles
Imaging

ABSTRACT

Biocompatible glutaraldehyde-cross-linked chitosan with new red fluorescence were prepared for the first time and were shaped into nanoparticles via inverse-microemulsion method. They could luminesce at ca. 670 nm either as powders and nanoparticles or in real and gelling solutions or suspensions, having a lifetime of 1.353 ns and a quantum yield of 0.08 in solution or 0.01 in solid state. The new-formed pyridinium structures and the intramolecular charge transfer effect are considered to be responsible for the new red emission, which have been proved by FTIR, ^{13}C NMR, and some calculation using Gaussian 09, respectively. Strikingly, they are quite inert and anti-photobleaching, with only <3% loss of fluorescent intensity per minute in average under a continuous laser illumination at 633 nm and 50 μW. Especially, their nanoparticles (5.6 nm) could enter into the negative nucleoli of living HeLa cells with low cytotoxicity for high contrast imaging inspections.

1. Introduction

Red luminescent materials are important indicators or imaging agents in the research fields of biomedicine and life sciences (Peng et al., 2011; Yake, Zahr, Jerri, Pishko, & Velegol, 2007; Zhu et al., 2011), because their red emission can penetrate deeper into biological systems, keep away the interference of bio-autofluorescence and decrease the scale of light scattering (Wu et al., 2011). As a consequence, high contrast optical images of cells, organs and even bodies can easily be traced. Up to now, molecular dyes like cyanines (such as Cy5 and Cy7) are on the top of usage (Yang et al., 2007). They are, however, expensive and have the shortage of photobleaching. Red luminescent quantum dots and upconversion nanoparticles were then explored to strengthen and lengthen the emission (Kumar, Srivastav, & Dutta, 2013; Mansur, Mansur, Curti, & De Almeida, 2012; Wang & Liu, 2009). Nevertheless, these inorganic nanoparticles are not very biocompatible, needing complicated modification and/or functionization before usage (Mahto, Park, Yoon, & Rhee, 2010; Su et al., 2010). Otherwise, they are prevented from direct applications to biological systems because of their potential toxicity. Other types of biocompatible red luminescent materials have hence been studied, of which some natural polymers have drawn a great attention because they possess diverse features including easy modification and biocompatibility (Evertsson & Nilsson, 1999; Kondaveeti, Prasd, & Siddhanta, 2013; Ye, Xiong, & Sun, 2012).

Among the studied natural polymers, chitin looks to be very attractive. It is commonly extracted from crustacean shells at high production but low cost, being now the second most abundant polysaccharides (just after cellulose). Chitosan, the linear (1-4)-2-amino-2-deoxy-β-D-glucan, commonly with degree of acetylation close to 0.20, is currently isolated from marine chitin (Muzzarelli, 2012; Muzzarelli et al., 2012). As non-toxic, biocompatible and biodegradable biopolymers, chitosan and its derivatives have been explored fairly extensively as drug carriers for biomedical and pharmaceutical applications (Anitha et al., 2011; Larsson et al., 2013; Muzzarelli, 2009a, 2009b; Shukla, Mishra, Arotiba, & Mamba, 2013; Silva, Caridade, Mano, & Reis, 2013). Therefore, it would be really interesting to verify if chitosan can be made into red luminescent biomaterials.

Chitosan itself can luminesce at ca. 450 nm which can be enhanced after being heated due to the formation of micelle structures (Huang et al., 2013). This fluorescence is however not far enough away from the bio-autofluorescence. In order to shift the fluorescence to a longer wavelength, Wei et al. have cross-linked the chitosan with formaldehyde or glutaraldehyde and demonstrated that the products could emit new fluorescence at ca. 520

* Corresponding author at: Key Laboratory of Analytical Chemistry for Living Biosystems, Institute of Chemistry, Chinese Academy of Sciences, Zhongguancun North First Street 2, Beijing 100190, China. Tel.: +86 010 62618240; fax: +86 10 62559373.
E-mail addresses: wangke007@iccas.ac.cn (K. Wang), yuanxun@iccas.ac.cn (X. Yuan), guozhenp@iccas.ac.cn (Z. Guo), xujy@iccas.ac.cn (J. Xu), chenyi@iccas.ac.cn (Y. Chen).

0144-8617/$ – see front matter © 2013 Elsevier Ltd. All rights reserved.
http://dx.doi.org/10.1016/j.carbpol.2013.10.100

and 580 nm besides the band at 450 nm (Wei et al., 2007, 2008). The band at 580 nm is clearly a red light but still not ideally away from the region of bio-autofluorescence if compared with Cy5. The anti-photobleaching ability of these cross-linked chitosan remains unclear yet.

To further shift the luminescence upwards to a band at least close to that of Cy5, the crosslinking reaction was re-explored in this laboratory and some new products able to emit a longer wavelength of red fluorescence were prepared by a few different ways. In this paper, a different method is introduced for preparing the new red luminescent cross-linked chitosan, that is, glutaraldehyde-based cross-linked chitosan (GCC). The reaction was performed at different concentrations of glutaraldehyde in acidic aqueous solutions or inverse microemulsions (for preparation of GCC nanoparticles or GCC NPs) (Liu, Shao, Ge, & Chen, 2007) rather than neutral or even basic solutions, and new GCC were obtained that could emit one strong fluorescence at ca. 670 nm (similar to Cy5) and two weak bands at ca. 615 and 575 nm. The strong red fluorescence was observed not only in real solutions and suspensions but also from gels and solid powders. More importantly, they had anti-photobleaching ability which is much superior to molecular dyes and somewhat similar to quantum dots. Furthermore, the GCC NPs could image the nucleoli of living HeLa cells with high contrast and low cytotoxicity.

2. Materials and methods

2.1. Materials

Chitosan (at a viscosity-averaged molecular weight, Mv, of ca. 50 kDa and deacetylation degree of 95.37%) and low molecular weight chitosan (Mv < 10 kDa and deacetylation degree = 85.24%) were purchased from Jinan Haidebei Marine Bioengineering Co., Ltd., Shandong, China. Glutaraldehyde (50 wt%, d = 1.12 g/ml, Mw = 100.2 Da) was from Sinopharm Chemical Reagent Co., Ltd., Beijing, China. Octanol was from Xilong Chemical Corporation, Shantou, China. Sylgard 184 silicone elastomer and curing agent for preparing polydimethylsiloxane (PDMS) were obtained from Dow Corning Corporation, Midland-Michigan, USA. Water-soluble Cy5, foetal bovine serum (FBS), Dulbecco's Modified Eagle Medium (DMEM), trypsin-EDTA solution and penicillin streptomycin were all from Invitrogen Co., California, USA; acetic acid, sulphuric acid, sodium borohydride, sodium hydroxide, iodine, potassium iodide and cyclohexane from Beijing Chemical Co., Beijing, China; while Triton X-100, phosphate buffered saline (PBS) and 3-(4,5-dimethylthiazolyl-2)-2,5-diphenyltetrazolium bromide (MTT) from Beijing Biodee Biotechnology Co., Ltd., Beijing, China. All the chemicals were analytical reagents and used as received. Dialysis bags of MD 34 (3500) were purchased from Union Carbide Co., Connecticut, USA. Distilled water was used throughout the study.

2.2. Preparation of GCC solution

Chitosan dissolved in 1.5% (v/v) acetic acid at 2 wt% was mixed with glutaraldehyde (0.01–1%) at an equal volume ratio. After sonication for 3–5 s, the mixed solution was left to react at room temperature (~25 °C) until its colour changed to orange under ambient light (ca. 20 h). The products were collected by dialysis against water for 2 days and dried by lyophilization for 2 days. The harvested bulk solid gels were used or stored directly or after they were ground into powders and/or re-dissolved in water.

2.3. Preparation of GCC gel

Chitosan dissolved in 1.5% (v/v) acetic acid at 2 wt% was mixed with glutaraldehyde (1–10%) at an equal volume ratio. After sonication for 3–5 s, the mixed solution was left to react at room temperature (~25 °C) until its colour changed to orange or dark orange under ambient light (ca. 20 h). The products were collected by dialysis against water for 2 days and dried by lyophilization for 2 days. The harvested bulk solid gels were used or stored directly or after they were ground into powders and/or re-dispersed in water.

2.4. Preparation of GCC NPs

Under vigorous stirring at about 700 rpm, the chitosan and glutaraldehyde solutions (5–10%) were mixed at a volume ratio of 1:1 at 0 °C in an ice/water bath, and into each volume of the aqueous phase was quickly added 4 volumes of a premixed solution of 7:8:9 (v/v/v) Triton X-100, octanol and cyclohexane. The mixture was sonicated at about 5 °C until it became transparent (commonly less than 10 min when water-in-oil microemulsions were formed). It was then warmed up to room temperature to accelerate the reaction and kept for about 20–30 h until the colourless solution changed to transparent dark orange under natural light. It was further mixed with ethanol/water (1:2, v/v) solution at a volume ratio of 1:3 and sonicated for less than 5 min to destroy the microemulsions. The oil phase was removed from the water phase after separation by centrifugation at 5000 rpm (1686 × g) for 10 min, and spherical GCC NPs were harvested from the water phase after dialysis and lyophilization. The GCC NPs can be stored, for at least one year, as dried powders or aqueous suspensions.

2.5. Selective reduction of GCC

The synthesized GCC NPs were first added into 0.1 M sodium hydroxide at about 5 mg/mL, then mixed with 0.5% $NaBH_4$ at a ratio of about 1:1 (v/v) and stirred at room temperature (~25 °C) for 24 h until the solution turned gradually from light yellow to colourless.

2.6. Quenching experiment

A solution of iodine (2 mmol/mL or 5 mg in 600 μL sulphuric acid) was first mixed in dark with 400 μL of 12 mg/mL aqueous potassium iodide, and further added with 1 mL of 2% GCC (commonly cross-linked with 1% glutaraldehyde) solution. After shaken for 1–5 min, the final solution was subjected to fluorescence spectroscopic measurement.

2.7. Characterization of GCC and GCC NPs

UV–vis absorption spectra, emission spectra and Fourier transform infrared (FTIR) spectra were recorded on spectrophotometer (TU-1900, Purkinje, China) using 1-cm quartz cuvettes, fluorophotometer (RF-5301PC, Shimadzu, Japan) and Fourier transform spectrophotometer (Spectrum 782, Perkin-Elmer, America), respectively. Solid-state ^{13}C nuclear magnetic resonance measurements were performed on Bruker 400 MHz machine (Bruker AV ANCE III, Bruker, USA) operated via cross polarization magic angle spinning (CP/MAS) at 100 MHz. The spectra were recorded at 3 ms contact time and 3 s delay time.

Emission lifetime was measured using Combined Fluorescence Lifetime and Steady State Spectrometer (FLS920, Edinburgh, England) mounted with two monochromators of model M300, one F900 nanosecond pulsed flash lamp and one single photon photomultiplier of model R928P. One of the monochromators was used for excitation at 630 nm and the other for emission at 670 nm. The lamp worked with H_2 filled at 1.1 atm pressure, 40 kHz and 1 ns FWHM pulse duration. The detected data were treated by the accompanied software EAI F900, version 6.2.3.

The quantum yield of aqueous solutions was measured using Cy5 (quantum yield 0.27 at 649 nm) as a standard (Schobel, Egelhaaf, Brecht, Oelkrug, & Gauglitz, 1999), and that of powder products was measured by NanoLog infrared fluorescence spectrometer (Nanolog FL3-2iHR, Horib Jobin Yvon, France) with an integrating sphere.

GCC NPs were imaged by transmission electron microscopy (TEM) on JEM 1011 (JEOL, Japan) at an accelerating voltage of 100 kV and a magnification rate of 50,000. The imaging samples were prepared by dropping aqueous dispersed NPs on a carbon-coated copper grid and completely dried by natural evaporation.

The size distribution and zeta potential (ζ) of GCC NPs were measured by a Zetasizer Nano instrument (ZEN3600, Malvern, England) with dynamic light scattering (DLS) software.

2.8. Cell imaging and in-cell/off-cell anti-photobleaching test

HeLa cells were grown at 37 °C on glass-bottom culture dishes from MatTek (Massachusetts, USA) in DMEM supplemented with 10% (v/v) FBS, 100 μg/mL penicillin and 100 μg/mL streptomycin. Two hours before usage, the cells were transferred into FBS-free

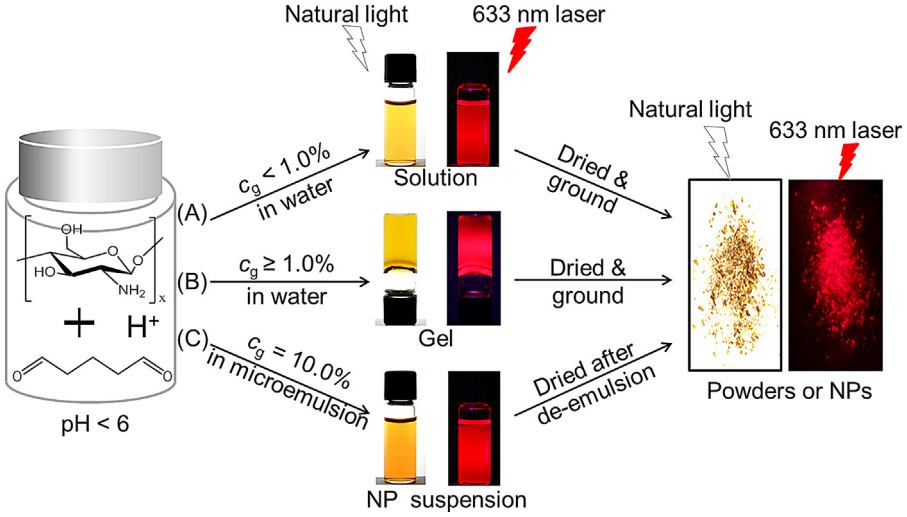

Scheme 1. Routes for preparation of red fluorescent GCC.

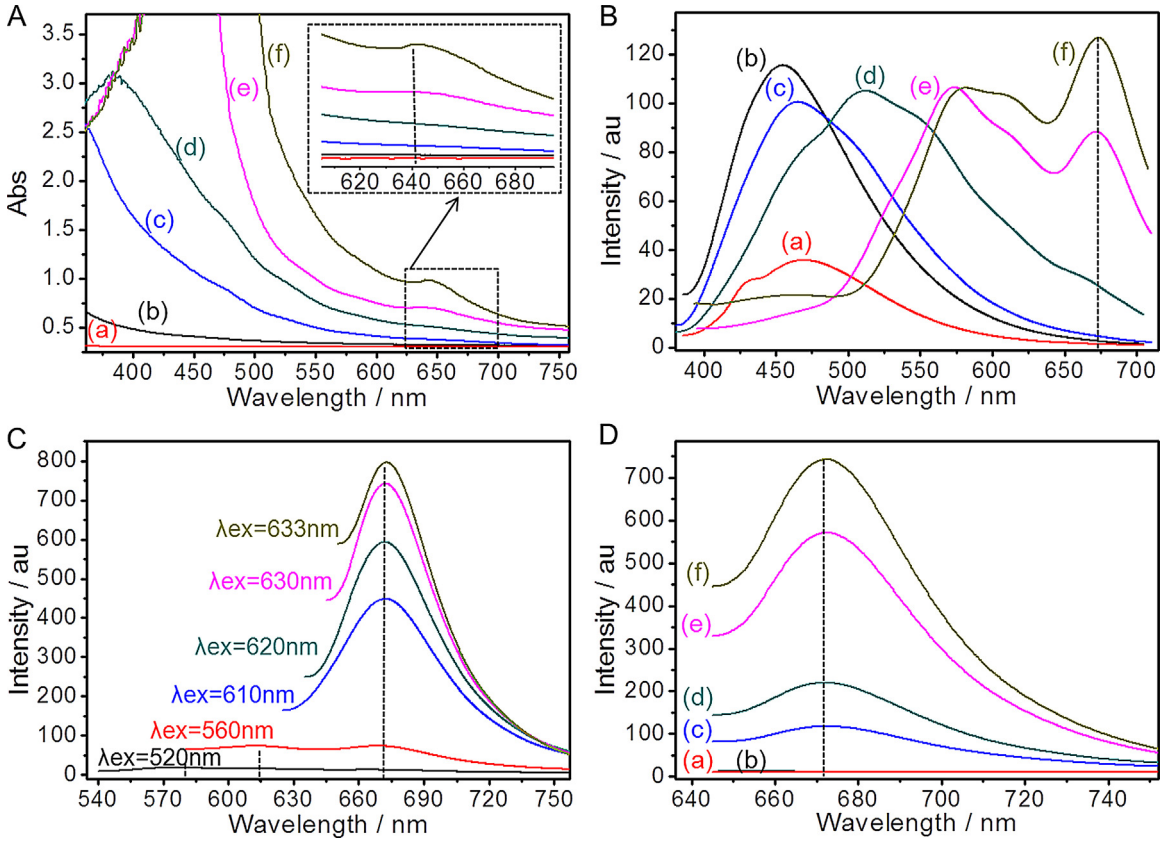

Fig. 1. (A) UV–vis absorption and (B and D) emission spectra of (a) glutaraldehyde, (b) chitosan and GCC at c_g of (c) 0.5%, (d) 1%, (e) 5% and (f) 10%, with the excitation wavelengths of 365 nm in (B) and 630 nm in (D), respectively; (C) emission of GCC formed at c_g of 10% under different excitation wavelengths. The excitation/emission slits in (B) are (a–c) 5/5, (d) 10/10, (e and f) 15/15 nm and the excitation/emission slits in (C and D) are 1.5/3 nm.

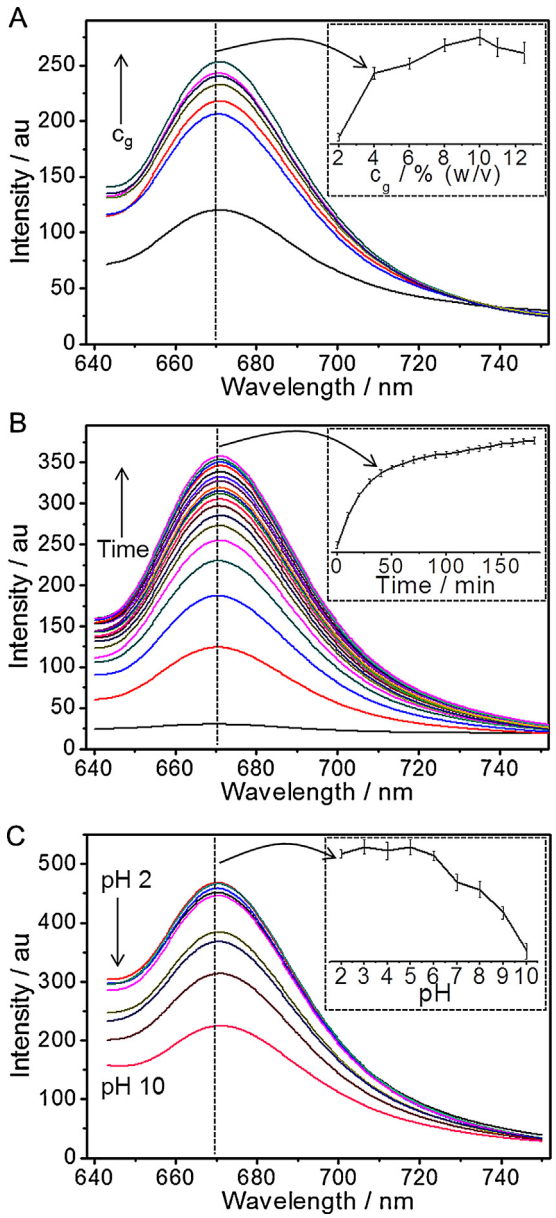

Fig. 2. Impact of (A) c_g, (B) reaction time and (C) pH on the emission of (A and B) GCC and (C) GCC NPs. The insets are their intensity at 670 nm against different (A) c_g, (B) reaction time and (C) pH.

DMEM and cultured at 37 °C for 50 min. An aqueous dispersion of 30 μg/mL GCC NPs was added to the dishes. After further incubation at 37 °C for 50 min, the NPs-tagged HeLa cells were imaged immediately on a confocal laser scanning microscope (FV1000, Olympus, Japan). A 100× objective lens and excitation of 633 nm laser line were selected. The in-cell anti-photobleaching of the NPs was performed by continuously irradiating the cells for at least 30 min. The optical intensity was rerecorded every 1 min and plotted against time.

The off-cell anti-photobleaching experiments were conducted by embedding a target reagent (GCC NPs, Cy5 or CdTe quantum dots) in PDMS and recording the emission on the same confocal laser scanning microscope. The embedding was achieved by first mixing PDMS monomer solution with its curing agent at a volume ration of 10:1, then with 1 volume of sample. After thoroughly degassed, the mixture was dropped on a clean glass slide and kept in an oven at 70 °C for ca. 1 h to complete polymerization. The slide was continuously irradiated under a laser (633 nm for GCC and Cy5 or 488 nm for quantum dots) for at least 30 min and the optical intensities were recorded every 1 min.

2.9. Cell viability

The viability of HeLa cells was tested by MTT assay (Lin, Cao, Chen, Wu, & Li, 2013; Zhang et al., 2013). HeLa cells were seeded in 35 wells (7 groups or 5 wells each group) on a 96-well plate (Corning Incorporated, New York, America) at a density of 7×10^4 cells/mL in DMEM and incubated for 18 h. The cells were then incubated with GCC NPs in DMEM for 24 h by replacing the used DMEM in each group (5 neighbouring wells) with 0, 10, 20, 30, 40, 50 and 60 μg/mL GCC NPs, respectively. All the wells were washed twice with PBS buffer and then added with freshly prepared 0.5 mg/mL MTT in DMEM. After incubation for 4 h, the left MTT in DMEM was removed by carefully sucking. The purple formazan crystals formed by the living cells was dissolved by addition of 150 μL DMSO into each well and gently shaken for ca. 10 min at room temperature. The absorbance of each well was then measured at 490 nm on a microplate reader (SpectraMax M5, Molecular Devices, USA), and the cell viability was calculated by dividing the 5-well averaged absorbance of NPs-incubated cells over that of the incubated cells without the addition of GCC NPs.

3. Results and discussion

3.1. Routes for preparation of GCC in different states

There are at least three potential routes that can be conceived for the preparation of powdered GCC, i.e. through solution, gel and NP suspension as illustrated in Scheme 1. These routes were demonstrated to be realizable by simply adjusting the added concentration of glutaraldehyde, c_g, and by selecting the amination degree and molecular weight of chitosan when the synthesis proceeded in an acidic solution. Chitosan with 95.37% deacetylation (i.e. with high amination degree) and ca. 50 kDa molecular weight allowed the preparations of powdered GCC from real solution at $c_g < 1\%$ (Scheme 1A) or gel at $c_g > 1\%$ (Scheme 1B) and GCC NPs at $c_g = 10\%$ (Scheme 1C). If the chitosan has a degree of deacetylation at ca. 85% and molecular weight lower than 10 kDa, only the first route (Scheme 1A) was practically available even at $c_g \gg 1\%$.

All the reactions were designed to start from acidic solutions at pH 3–5 in order to suppress the isomerization and self-polymerization of glutaraldehyde, which can exist in much simpler forms in acidic conditions than in neutral or basic environments (Pratta, Wilsona, & Kozinskib, 2013), and assist to synthesis the target products. Taking this as a prerequisite, all the reaction routes were designed to be achieved in one-pot preparation, including the use of microemulsions to serve as micro reactors (Scheme 1C).

The solubility of the dried GCC was shown to be different. The real-solution-solidified products could be re-dissolved in water at room temperature but the gel products were not or dependent on how they were synthesized. For example, the GCC gels obtained at $c_g = 1\%$, with the degree of cross-linking (estimated as the amount of glutaraldehyde divided by the total amount of glutaraldehyde and chitosan) at ca. 0.05%, were capable of returning to solutions after they were finely powdered and stirred in water at 60 °C and 1000 rpm for ca. 1 h; but those products synthesized at $c_g = 10\%$, with the degree of cross-linking at ca. 0.5%, could not be re-dissolved in water even after their powders were stirred and heated for >3 h. However, all the powdered GCC could well be suspended in water due to their high hydrophilicity, which makes them highly biocompatible.

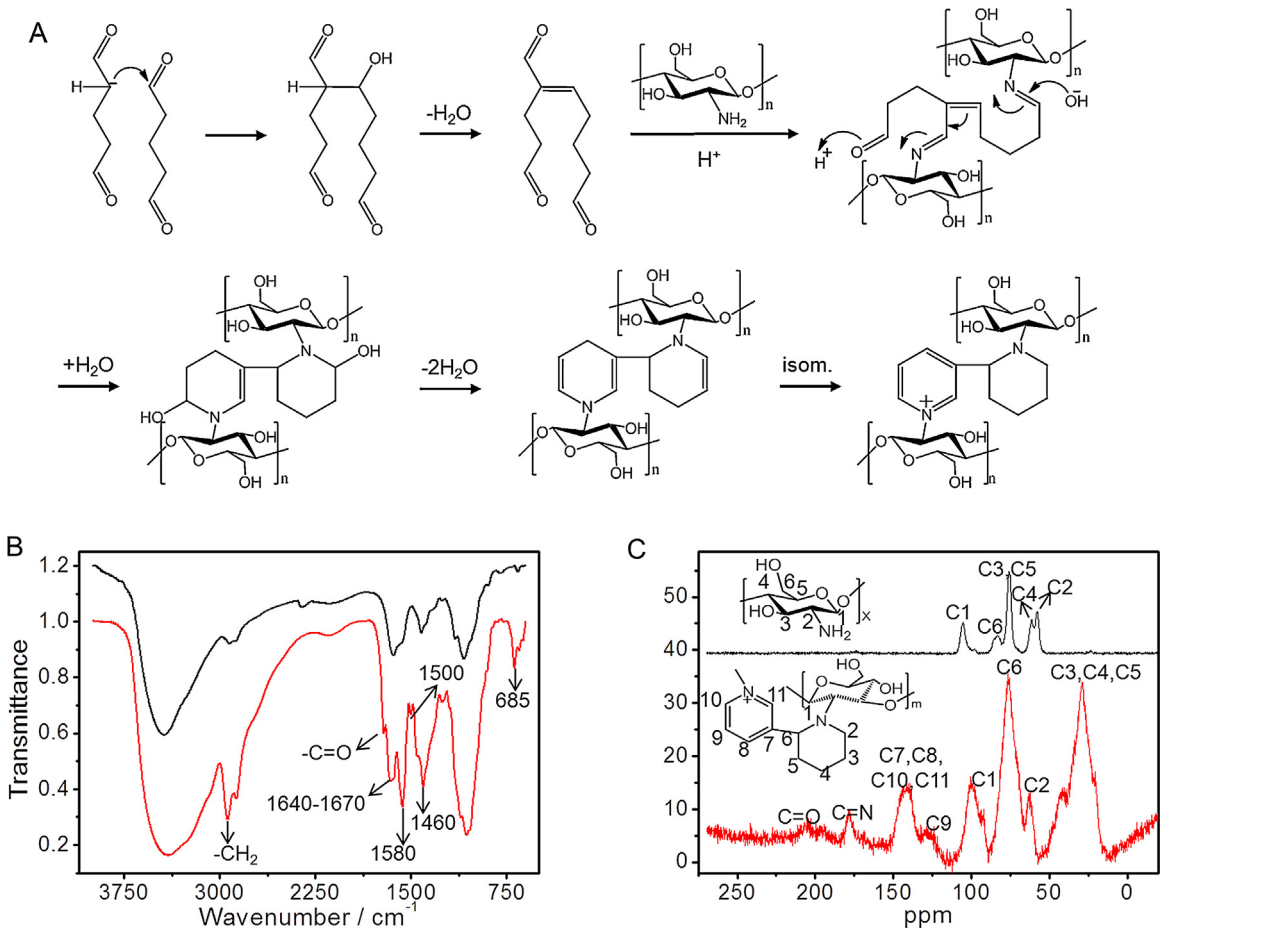

Fig. 3. (A) Reaction mechanism of forming pyridinium structures between chitosan and glutaraldehyde; (B) Fourier transform infrared and (C) ^{13}C NMR spectra of chitosan (the upper line) and GCC (the lower line).

In brief, this method offers a simple way to control the reaction and in turn the product states. This has been achieved by selection of chitosan molecular weight and amination degree, and especially the concentration of glutaraldehyde. Further regulation of the products lies in the solidification and re-dissolution of the solid products. The method is extendable to the synthesis of other types of glutaraldehyde-cross-linked amines (data not shown), not limit to chitosan and low molecular weight chitosan. The operation of the method is easy, requiring only mixing up glutaraldehyde at a given concentration with a selected chitosan or other amines in acidic water and harvesting the products by purifying them via dialysis. The preparation of GCC is very economic by using the abundant and cheap reactant of chitosan.

3.2. Luminescent property

All the prepared GCC could emit red light in all the physical states as shown in Scheme 1, the right photos. Their detailed absorption and emission spectra were collectively illustrated in Fig. 1. The striking feature is that, during formation of GCC, some new absorption peaks appeared (the longest one at ca. 640 nm) and the intensity increased with c_g (Fig. 1A), accompanied by a gradual shift of emission from about 450 nm (produced by chitosan and/or glutaraldehyde) to ca. 670 nm (Fig. 1B). Further check revealed that the longest emission is at ca. 670 nm, and GCC could easily be excited by a wide wave band below 650 nm (Fig. 1C). For convenience, we preferred to select either 630 or 633 nm (He-Ne laser) as the excitation wavelength (Fig. 1D). For most biological applications, the emission at ca. 670 nm is highly preferred, which can more effectively avoid the interference of biological autofluorescence. The synthesized GCC with strong 670 nm emission have a quantum yield of 0.08 in solution or 0.01 in solid state.

Detailed measurement showed that c_g had an upward asymptotic contribution to the emission of GCC as shown in Fig. 2A, which demonstrated that the luminescence intensity grown with the degree of cross-linking. This may provide a way to control the intensity of their emission. Similarly, the emission also increased with reaction time as shown in Fig. 2B, with a turning point at ca. 50 min. Besides, pH was shown to have a serious impact on the emission of GCC. Fig. 2C shows that the optical intensity is quite stable at pH 2–6 but starts to decrease quickly at pH > 6. This suggests that GCC have to be prepared at pH < 6. Here GCC NPs were used for the pH study because the pH value could be adjusted more conveniently in their NP solution state than in gel state.

3.3. Characterization and luminescence mechanism

The new red emissions suggest the existence of some new structures in GCC compared with other reported cross-linked chitosan. In common sense the reactions will result in the formation of Schiff's bases, so that in literatures the bands II (520 nm) and III (580 nm) were attributed to the n–π^* transitions of C=N bonds in the Schiff's bases, and the high-energy absorption of band I (between 420 and 480 nm) to the π–π^* transition of C=C double bonds (Wei et al., 2007, 2008). The emission wavelengths below 600 nm as showed in Fig. 1B were also consistent with above emission bonds, which could be explained by the same reason. However, these transitions look not suitable to explain the emission of fairly

long wavelengths (ca. 670 nm) in this study. A better mechanism to elucidate the emission may include some re-arrangements of the C=N and C=C bounds. In fact, it has been reported that further condensation and cyclization of the products were possible, resulting in the formation of pyridinium and hexahydropyridine ring structures on chitosan as shown in Fig. 3A, the so-called 'anabilysine' unit (Hardy, Hughes, & Rydon, 1979; Hardy, Nicholls, & Rydon, 1976; Migneault, Dartiguenave, Bertrand, & Waldron, 2004; Southern, Hughes, Lawford, Clench, & Manning, 2000). Compared with the cross-linking reactions which took placed in the surfaces of chitosan microspheres (Wei et al., 2007, 2008), in our method, chitosan can cross-linked with glutaraldehyde more thoroughly in the preparation of GCC, which will increase the degree of cross-linking and facilitate the formation of 'anabilysine' units in GCC and then endow GCC with new fluorescent properties.

The presence of pyridinium structures on GCC were characterized by Fourier transform infrared spectra and ^{13}C NMR spectra as shown in Fig. 3B and C, respectively. In the Fourier transform infrared spectrum of GCC (Fig. 3B, the lower line), some characteristic peaks of aromatic pyridine ring and/or pyridinium structure appear at 1460, 1500, 1580, 685 and 1640–1671 cm^{-1} (Xing, Xu, Zhou, & Pei, 1992), which are very significant in comparison with those of chitosan (Fig. 3B, the upper line). In addition, there were peaks from C=C and C=N overlapping the wider bands between 1640 and 1671 cm^{-1}. Similar information was also observed on the ^{13}C NMR spectra (Fig. 3C). Different from the spectrum of chitosan (Fig. 3C, the upper line), GCC shows its pyridinium structures by some featured peaks at 125–145 ppm which were overlapped with that of conjugated C=C bonds (Fig. 3C, the lower line), and C=N double bonds that conjugated with C=C by peaks at 178.30. The wide peaks at 25–45 ppm suggested the formation of $-CH_2$ in GCC (Monteiro & Airoldi, 1999; Xing et al., 1992).

There are further evidences to prove the contribution of pyridinium structures to the red emission. Firstly, by reduction of GCC solutions with sodium borohydride which can selectively reduce the pyridinium but not pyridine structures (Lyle & Boyce, 1974), the solutions changed its colour from light yellow to colourless under natural light, and the red emission at ca. 670 nm almost completely disappeared as shown in Fig. 4A. Secondly, the luminescence of pyridinium structures could strongly be affected by pH value because the pyridinium can be protonated or deprotonated as pH varies. This has just been discussed as illustrated in Fig. 2C where the GCC NPs significantly reduce their emission intensity as the pH increases from pH 6 to pH 10. This also agrees well with the dissociation constant of pyridine ($pK_a = 5.17$). And thirdly, the Zeta potentials of the NPs were measured to decrease from +42.1 to +19.8 mV as pH increased from 4 to 10. It is known that the pyridinium structures cannot stably exist at a pH above 6 and will gradually change into pyridine, a non-luminescent structure. The change reduces the surficial positive charges on NPs and in turn the Zeta potentials.

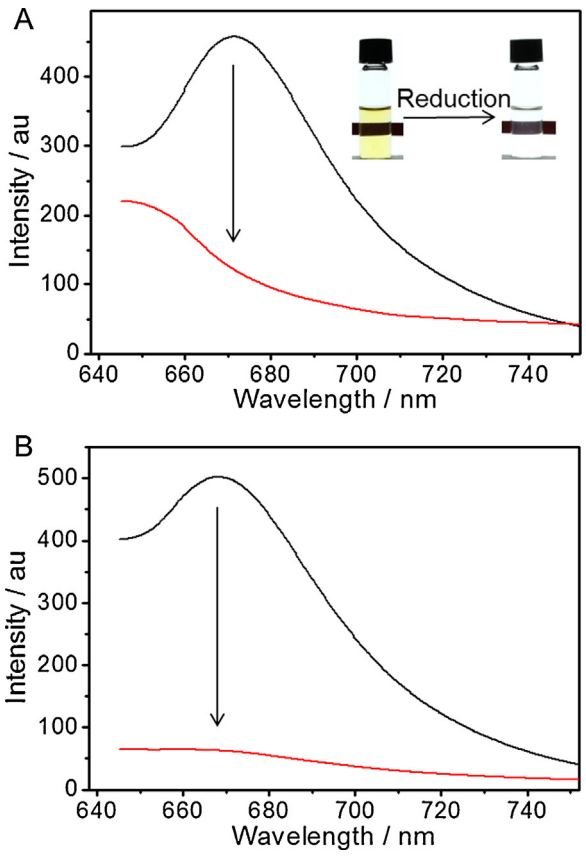

Fig. 4. Emission spectra of GCC solution with excitation wavelengths of 630 nm. (A) Before (the upper line) and after (the lower line) being selectively reduced by $NaBH_4$;
(B) Before (the upper line) and after (the lower line) being quenched by iodine.

The emission is certainly a fluorescence which could be statically quenched by iodine (Fig. 4B) (Fischer & Georges, 1998) and has a measured lifetime of 1.353 ns which suggests a direct electron transition from the singlet excited state to its ground state (Hong, Lam, & Tang, 2011). To better understand the nature of red fluorescence,

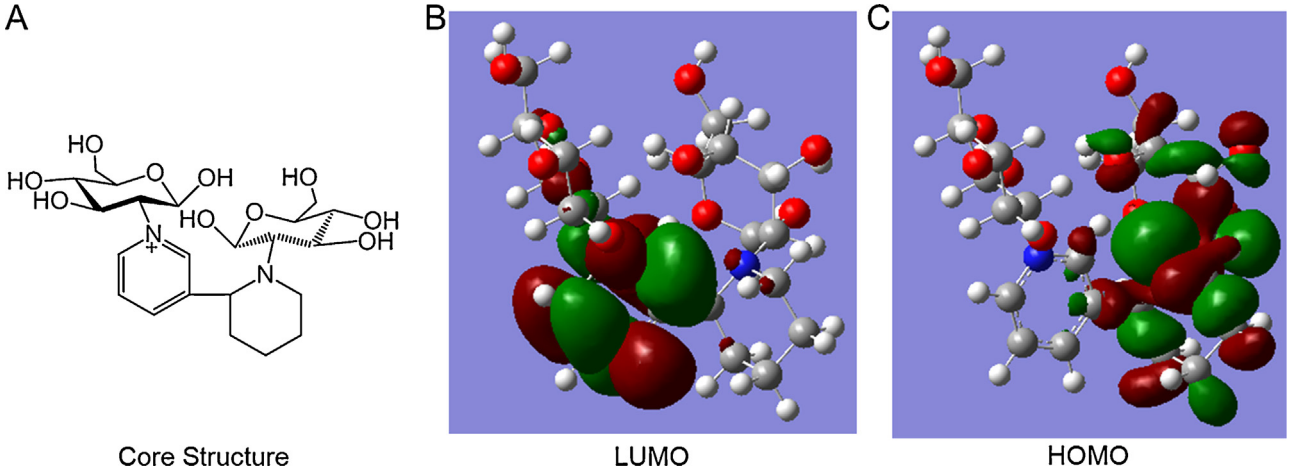

Fig. 5. Molecular structure of the GCC model compound and representation of the frontier orbitals (HOMO and LUMO) of the model compound.

quantum chemical optimization on their energy levels based on density functional theory with B3LYP hybrid functional theory at the basis set level of 6-31G(d) using Gaussian 09 was conducted (Frisch et al., 2009). In order to simplify the calculation, a very simple GCC model compound with only one pyridinium core structure (Fig. 5A) was chosen. The results illustrate that the electron clouds of LUMO are dominated by the electron-accepting structures of pyridinium (Fig. 5B), while those of HOMO are mainly on the electron-donating units of hexahydropyridine ring (Fig. 5C). Such an electron distribution can generally endow the molecules with an intrinsic intramolecular charge transfer property and luminescent property (Yuan et al., 2012).

It looks certain that the pyridinium structures are the core structures and the intramolecular charge transfer effect assists the bathochromic effect which endows GCC with the longer fluorescent emission. However, a full understanding of the emission mechanism needs a more systematic study and has to be discussed elsewhere.

3.4. Imaging the nucleoli of living HeLa cells

The red luminescent GCC were shown to be highly stable or inert. They could be stored for more than one year under the ambient light at room temperature, with only about 20% loss of fluorescence. A more favourable feature is that they could sustain a long time (at least 30 min) of continuous laser excitation in either cells or PDMS, with only less than 30% loss of emission intensity at 50 μW (Fig. 6B), much better than that of fluorescent molecule of Cy5 (Fig. 6D) and even approaching the CdTe quantum dots which had also a loss of about 30% at the excitation laser energy of 140 μW (Fig. 6A). It should be noted that the fluorescent loss of GCC in PDMS could be elevated up to 50% at a high laser power of 213 μW (Fig. 6C) but this may not affect too much on their applications because strong laser is generally avoided in bioanalysis for safe reasons.

By taking the advantages of strong anti-photobleaching ability and good hydrophilicity, GCC could be an ideal type of biological imaging reagents. This was strengthened by their low cytotoxicity

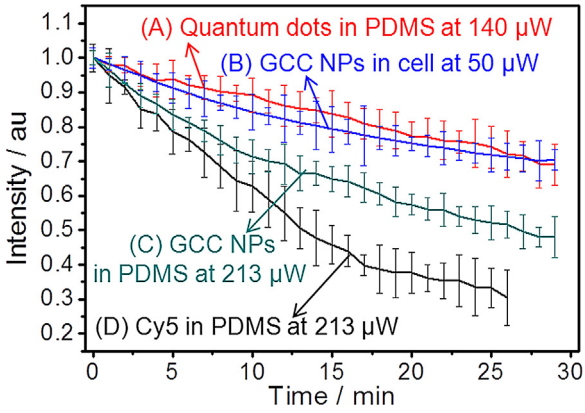

Fig. 6. Photobleaching spectra. (A) CdTe quantum dots excited at 488 nm and 140 μW; (B) GCC NPs in HeLa cells excited at 633 nm and 50 μW; (C) GCC NPs in PDMS excited at 633 nm and 213 μW; (D) Cy5 excited at 633 nm and 213 μW.

which was evaluated by MTT assay through incubation of living HeLa cells with 5.6 nm GCC NPs (Fig. 7A and B). At a concentration up to 60 mg/L GCC NPs, the cells were viable at a rate higher than 75% (Fig. 7C).

The applicability of GCC to cell imaging was validated by confocal microscopy of HeLa cells with the same 5.6 nm GCC NPs (Fig. 7D) as a fluorescent probe. At a size similar to bovine serum albumin, the NPs could easily enter into the cells (in less than 50 min) and were sustainable to clearness of the reticuloendothelial system, which is different from those large nanoparticles (Davis, Chen, & Shin, 2008). This fast entrance was also attributed to the electrostatic attraction of the positively charged NPs and the negatively charged cells (Budin, Yang, Reiner, & Weissleder, 2011). Fig. 7D–F show that the NPs could aggregate around the negative charged cellular regions, especially the nucleoli, possibly being a new means to image the cellular nucleoli. This further highlights the value of GCC NPs because very few biocompatible luminescent reagents are presently available to trace the nucleoli of cells without complex accessorial strategies (Yue et al., 2011).

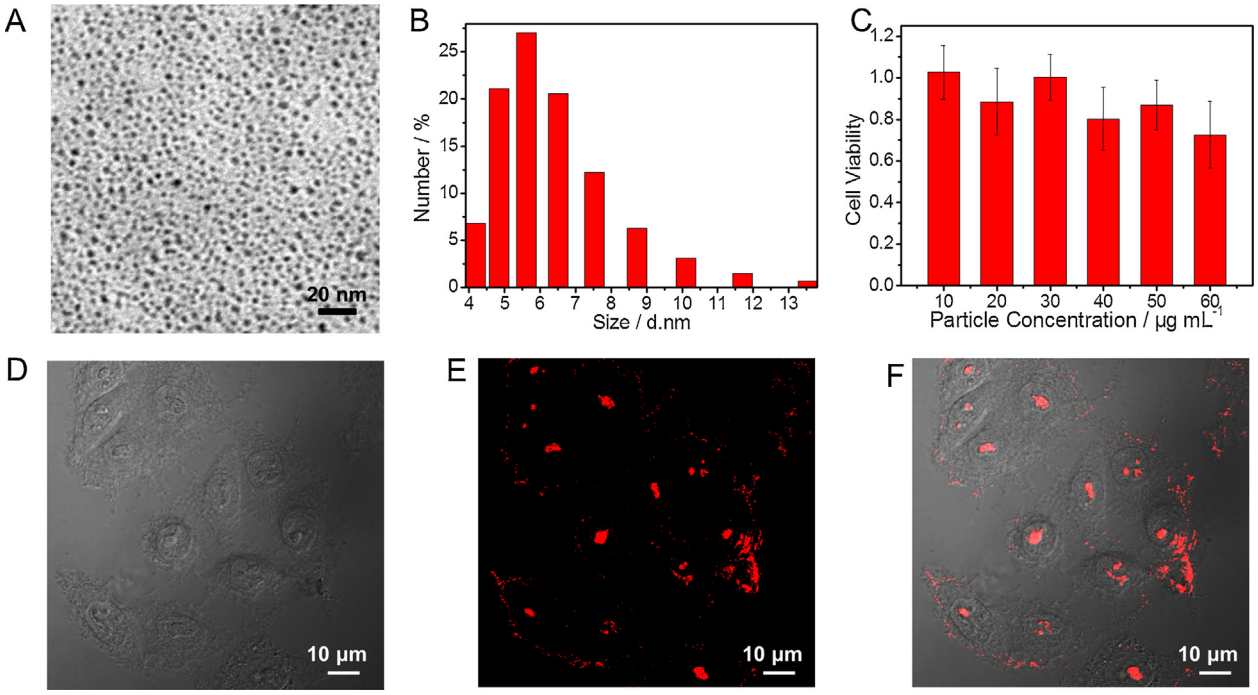

Fig. 7. (A) TEM image of GCC NPs; (B) their DLS spectrum with an average size of 5.6 nm; (C) viability of NPs-treated HeLa cells ($n = 5$); (D) the differential interference contrast image; (E) confocal laser scanning image and (F) merged image of D and E measured from HeLa cells after incubation with NPs.

This kind of NPs with low cytotoxicity, strong anti-photobleaching property and the unique feature to specifically image the negative region of cells may become an excellent optical probe at least in cell analysis. They can also be further modified to extend their applications, for instance, serving as traceable drug carriers, because they contain many free reactive groups (e.g. hydroxyl groups and amino groups).

4. Conclusions

In summary, an elegant method has been established for the robust preparation of a new type of red fluorescent GCC and GCC NPs. The preparation did not need extra heating accessories except for mixing chitosan and glutaraldehyde together or in microemulison at room temperature (25 °C). With pH < 6 and proper c_g, the GCC can all emit a red fluorescence at ca. 670 nm with a lifetime of 1.353 ns, no matter in which physical states (solution, gel, solidified powder or NPs), although the quantum yields varied, 0.08 in solutions and 0.01 for solid powders. The pyridinium structures and intramolecular charge transfer effect can help to explain the new red emission from GCC. The prepared GCC are highly hydrophilic and could be stored in ambient surroundings for a long time. The most attractive features are that they can sustain at least 30 min laser irradiation and have low cytotoxicity. Especially, the GCC NPs are highly water-dispersible, having a diameter of 5.6 nm and able to easily and fast enter into the living HeLa cells to produce high contrast and high resolution images of cellular nucleoli. It is also very important that GCC NPs can further be functionalized with free reactive groups on them and can potentially be used in medicine for simultaneously lighting up the nucleoli of tumour cells and delivering anticancer drugs. Such a type of luminescent GCC and GCC NPs may open a new door to prepare multifunctional materials useful in biomedicine-related fields.

Acknowledgement

We thank the donation of HeLa cells from Prof. L. Q. Mao and gratefully acknowledge the financial support from NSFC (Nos. 21027003 and 21235007), MOST (Nos. 2012IM030900 and 2012IM030400) and CAS.

References

Anitha, A., Deepa, N., Chennazhi, K. P., Nair, S. V., Tamura, H., & Jayakumar, R. (2011). Development of mucoadhesive thiolated chitosan nanoparticles for biomedical applications. *Carbohydrate Polymers*, *83*, 66–73.

Budin, G., Yang, K. S., Reiner, T., & Weissleder, R. (2011). Bioorthogonal probes for polo-like kinase 1 imaging and quantification. *Angewandte Chemie International Edition*, *50*, 9378–9381.

Davis, M. E., Chen, Z., & Shin, D. M. (2008). Nanoparticle therapeutics: An emerging treatment modality for cancer. *Nature Reviews Drug Discovery*, *7*, 771–782.

Evertsson, H., & Nilsson, S. (1999). Microstructures formed in aqueous solutions of a hydrophobically modified nonionic cellulose derivative and sodium dodecyl sulfate: A fluorescence probe investigation. *Carbohydrate Polymers*, *40*, 293–298.

Fischer, M., & Georges, J. (1998). Limitations arising in the study of the fluorescence quenching of rhodamine 6G by iodides using cw-laser thermal lens spectrometry. *Spectrochimica Acta, Part A*, *54*, 101–110.

Frisch, M. J., Trucks, G. W., Schlegel, H. B., Scuseria, G. E., Robb, M. A., Cheeseman, J. R., et al. (2009). *Gaussian 09, Revision A02*. Wallingford, CT: Gaussian, Inc.

Hardy, P. M., Hughes, G. J., & Rydon, H. N. (1979). The nature of the cross-linking of proteins by glutaraldehyde. Part 2. The formation of quaternary pyridinium compounds by the action of glutaraldehyde on proteins and the identification of a 3-(2-piperidyl)-pyridinium derivative, anabilysine, as a cross-linking entity. *Journal of the Chemical Society, Perkin Transactions 1*, 2282–2288.

Hardy, P. M., Nicholls, A. C., & Rydon, H. N. (1976). The nature of the cross-linking of proteins by glutaraldehyde. Part 1. Interaction of glutaraldehyde with the amino-groups of 6-aminohexanoic acid and of α-N-acetyl-lysine. *Journal of the Chemical Society, Perkin Transactions 1*, *9*, 958–962.

Hong, Y., Lam, J. W. Y., & Tang, B. Z. (2011). Aggregation-induced emission. *Chemical Society Reviews*, *40*, 5361–5388.

Huang, H. W., Liu, F., Chen, S. N., Zhao, Q., Liao, B., Long, Y. F., et al. (2013). Enhanced fluorescence of chitosan based on size change of micelles and application to directly selective detecting Fe^{3+} in human serum. *Biosensors and Bioelectronics*, *42*, 539–544.

Kondaveeti, S., Prasad, K., & Siddhanta, A. K. (2013). Functional modification of agarose: A facile synthesis of a fluorescent agarose-tryptophan based hydrogel. *Carbohydrate Polymers*, *97*, 165–171.

Kumar, H., Srivastava, R., & Dutta, P. K. (2013). Highly luminescent chitosan-l-cysteine functionalized CdTe quantum dots film: Synthesis and characterization. *Carbohydrate Polymers*, *97*, 327–334.

Larsson, M., Huang, W. C., Hsiao, M. H., Wang, Y. J., Nyden, M., Chiou, S. H., et al. (2013). Biomedical applications and colloidal properties of amphiphilically modified chitosan hybrids. *Progress in Polymer Science*, *38*, 1307–1328.

Lin, Z., Cao, S., Chen, X., Wu, W., & Li, J. (2013). Thermoresponsive hydrogels from phosphorylated ABA Triblock copolymers: A potential scaffold for bone tissue engineering. *Biomacromolecules*, *14*, 2206–2214.

Liu, G. G., Shao, L., Ge, F., & Chen, J. F. (2007). Preparation of ultrafine chitosan particles by reverse microemulsion. *China Particuology*, *5*, 384–390.

Lyle, R. E., & Boyce, C. B. (1974). Sodium borohydride reduction of sterically hindered pyridinium salts. *Journal of Organic Chemistry*, *39*, 3708–3711.

Mahto, S. K., Park, C., Yoon, T. H., & Rhee, S. W. (2010). Assessment of cytocompatibility of surface-modified CdSe/ZnSe quantum dots for BALB/3T3 fibroblast cells. *Toxicology in Vitro*, *24*, 1070–1077.

Mansur, H. S., Mansur, A. A. P., Curti, E., & De Almeida, M. V. (2012). Bioconjugation of quantum-dots with chitosan and N,N,N-trimethyl chitosan. *Carbohydrate Polymers*, *90*, 189–196.

Migneault, I., Dartiguenave, C., Bertrand, M. J., & Waldron, K. C. (2004). Glutaraldehyde: Behavior in aqueous solution, reaction with proteins, and application to enzyme crosslinking. *Biotechniques*, *37*, 790–802.

Monteiro, O. A. C., Jr., & Airoldi, C. (1999). Some studies of crosslinking chitosan–glutaraldehyde interaction in a homogeneous system. *International Journal of Biological Macromolecules*, *26*, 119–128.

Muzzarelli, R. A. A. (2009a). Chitins and chitosans for the repair of wounded skin, nerve, cartilage and bone. *Carbohydrate Polymers*, *76*, 167–182.

Muzzarelli, R. A. A. (2009b). Genipin-crosslinked chitosan hydrogels as biomedical and pharmaceutical aids. *Carbohydrate Polymers*, *77*, 1–9.

Muzzarelli, R. A. A. (2012). 10.06 – Nanochitins and nanochitosans, paving the way to eco-friendly and energy-saving exploitation of marine resources. *Polymer Science: A Comprehensive Reference*, *10*, 153–164.

Muzzarelli, R. A. A., Boudrant, J., Meyer, D., Manno, N., DeMarchis, M., & Paoletti, M. G. (2012). A tribute to Henri Braconnot, precursor of the carbohydrate polymers science, on the chitin bicentennial. *Carbohydrate Polymers*, *87*, 995–1012.

Peng, X., Wu, T., Fan, J., Wang, J., Zhang, S., Song, F., et al. (2011). An effective minor groove binder as a red fluorescent marker for live-cell DNA imaging and quantification. *Angewandte Chemie International Edition*, *50*, 4180–4183.

Pratta, D. Y., Wilsona, L. D., & Kozinskib, J. A. (2013). Preparation and sorption studies of glutaraldehyde cross-linked chitosan copolymers. *Journal of Colloid and Interface Science*, *395*, 205–211.

Schobel, U., Egelhaaf, H. J., Brecht, A., Oelkrug, D., & Gauglitz, G. (1999). New donor–acceptor pair for fluorescent immunoassays by energy transfer. *Bioconjugate Chemistry*, *10*, 1107–1114.

Shukla, S. K., Mishra, A. K., Arotiba, O. A., & Mamba, B. B. (2013). Chitosan-based nanomaterials: A state-of-the-art review. *International Journal of Biological Macromolecules*, *59*, 46–58.

Silva, S. S., Caridade, S. G., Mano, J. F., & Reis, R. L. (2013). Effect of crosslinking in chitosan/aloe vera-based membranes for biomedical applications. *Carbohydrate Polymers*, *98*, 581–588.

Southern, L. J., Hughes, H., Lawford, P. V., Clench, M. R., & Manning, N. J. (2000). Glutaraldehyde-induced cross-links: A study of model compounds and commercial bioprosthetic valves. *Journal of Heart Valve Disease*, *9*, 241–248.

Su, Y., Hu, M., Fan, C., He, Y., Li, Q., Li, W., et al. (2010). The cytotoxicity of CdTe quantum dots and the relative contributions from released cadmium ions and nanoparticle properties. *Biomaterials*, *31*, 4829–4834.

Wang, F., & Liu, X. (2009). Recent advances in the chemistry of lanthanide-doped upconversion nanocrystals. *Chemical Society Reviews*, *38*, 976–989.

Wei, W., Wang, L. Y., Yuan, L., Wei, Q., Yang, X. D., Su, Z. G., et al. (2007). Preparation and application of novel microspheres possessing autofluorescent properties. *Advanced Functional Materials*, *17*, 3153–3158.

Wei, W., Yuan, L., Hu, G., Wang, L. Y., Wu, J., Hu, X., et al. (2008). Monodisperse chitosan microspheres with interesting structures for protein drug delivery. *Advanced Materials*, *20*, 2292–2296.

Wu, C., Hansen, S. J., Hou, Q., Yu, J., Zeigler, M., Jin, Y., et al. (2011). Design of highly emissive polymer dot bioconjugates for in vivo tumor targeting. *Angewandte Chemie International Edition*, *50*, 3430–3434.

Xing, Q. Y., Xu, R. Q., Zhou, Z., & Pei, W. W. (1992). *Fundamental organic chemistry* (2nd ed., pp. 352–354). Beijing: Higher Education Press.

Yake, A. M., Zahr, A. Z., Jerri, H. A., Pishko, M. V., & Velegol, D. (2007). Localized functionalization of individual colloidal carriers for cell targeting and imaging. *Biomacromolecules*, *8*, 1958–1965.

Yang, Z., Zheng, S., Harrison, W. J., Harder, J., Wen, X., Gelovan, J. G., et al. (2007). Long-circulating near-infrared fluorescence core-cross-linked polymeric micelles: Synthesis, characterization, and dual nuclear/optical imaging. *Biomacromolecules*, *8*, 3422–3428.

Ye, J., Xiong, J., & Sun, R. (2012). The fluorescence property of Schiff's bases of carboxymethyl cellulose. *Carbohydrate Polymers*, *88*, 1420–1424.

Yuan, W. Z., Gong, Y., Chen, S., Shen, X. Y., Lam, J. W. Y., Lu, P., et al. (2012). Efficient solid emitters with aggregation-induced emission and intramolecular charge transfer characteristics: Molecular design, synthesis, photophysical behaviors, and OLED application. *Chemistry of Materials*, *24*, 1518–1528.

Yue, Z. G., Wei, W., Lv, P. P., Yue, H., Wang, L. Y., Su, Z. G., et al. (2011). Surface charge affects cellular uptake and intracellular trafficking of chitosan-based nanoparticles. *Biomacromolecules*, *12*, 2440–2446.

Zhang, X., Zhao, J., Wen, Y., Zhu, C., Yang, J., & Yao, F. (2013). Carboxymethyl chitosan-poly(amidoamine) dendrimer core–shell nanoparticles for intracellular lysozyme delivery. *Carbohydrate Polymers*, *98*, 1326–1334.

Zhu, H., Liu, F., Guo, J., Xue, J., Qin, Z., & Gu, Y. (2011). Folate-modified chitosan micelles with enhanced tumor targeting evaluated by near infrared imaging system. *Carbohydrate Polymers*, *86*, 1118–1129.